

# Parawing Precision Aerial Delivery System

J. EVERETTE FOREHAND\*

*U.S. Army Aviation Materiel Laboratories, Fort Eustis, Va.*

AND

HERBERT Q. BAIR†

*Goodyear Aerospace Corporation, Akron, Ohio*

A gliding cargo-airdrop system that includes automatic homing and manual control has been developed. Theoretical and empirical data evolved during the development are presented. Data include a materials evaluation that considers critical parameters such as dimensional stability, packageability, maximum strength for minimum weight and volume, permeability, and the effects of humidity and temperature. Testing of reefing techniques and the establishment of the final reefing method as the optimum tradeoff between performance, simplicity, reliability, and cost are described. The establishment of control sensitivity is discussed; a 0.2 maximum degradation of the effective glide ratio due to control inputs of the automatic homing system was obtained. Validation of system performance characteristics and data correlation are described. System performance validation was obtained with manned jumps and with instrumented airdrops in both the automatic-homing and manual-control modes. Data correlation was obtained with onboard instrumentation, photography, radar tracking, Fairchild Analyzer, and closed-circuit television.

## Nomenclature

CEP	= circle of equal probability
IAS	= indicated air speed
$C_R$	= shock opening factor
$g$	= acceleration due to gravity, ft/sec <sup>2</sup>
$L_K$	= keel length, ft
$q$	= dynamic pressure, psf
$R$	= turning radius, ft
$S$	= wing area, ft <sup>2</sup>
$t$	= time to turn 360°, sec
$t_f$	= parawing inflation time, sec
$V$	= velocity, fps
$\phi$	= bank angle, deg

## Introduction

THE parawing precision aerial delivery system (PPADS) is an electronically guided gliding cargo-airdrop system that can deliver critical materials and supplies to troops in remote or hostile areas at any time of day or night under all kinds of weather and terrain conditions. Because the drop aircraft does not have to fly directly over the target area, the position of the cargo being supplied is not disclosed. The aircrew conducting the drop is also assured greater safety because the delivery aircraft can remain out of danger zones while making the drop.

The system, developed by Goodyear Aerospace for the U.S. Army Aviation Materiel Laboratories (USAAVLABS), Fort Eustis, Virginia, is capable of automatically delivering 100 to 500 lb of cargo to within 200 ft of a ground radio transmitter from altitudes of 500 to 30,000 ft.

Without payload, the system weighs approximately 100 lb and can be dropped from any cargo-carrying aircraft. The payload hits the ground with approximately the same impact as a parachute-dropped load, approximately 20 fps in vertical descent. Its horizontal velocity approaches 60 fps.

Presented as Paper 68-958 at the AIAA 2nd Aerodynamic Deceleration Systems Conference, El Centro, Calif., September 23-25, 1968; submitted November 18, 1968; revision received May 2, 1969.

\* Chief, Flexible Wing Branch, Aircraft Systems and Equipment Division. Member AIAA.

† Recovery Systems Engineer. Member AIAA.

It uses a delta-shaped steerable glider, the parawing, for a lifting surface (see Fig. 1). The parawing is constructed of urethane-coated nylon cloth. A control subsystem containing a radio receiver, logic circuits, servocontrol motor, and power supply is suspended between the parawing and the payload. The payload is attached beneath the control unit on a single-point swivel.

## Technical Discussion

### Aerodynamics

Several variables including the rigging line lengths, canopy planforms, payload configuration, and system geometry determine the highest lift-drag ratio (L/D) attainable by a parawing system. Testing has indicated a direct correlation between maximum L/D and maximum response sensitivity to control forces and movement.

Limited wind-tunnel tests of the parawings (see Fig. 2) conducted in the Langley Research Center full-scale tunnel indicated a 22% greater L/D for the twin-keel parawings compared to the single-keel parawings. The catenary keel panels also appeared to produce a more stable parawing with less sideslip. Data were taken at wind speeds from 35 to 60 fps

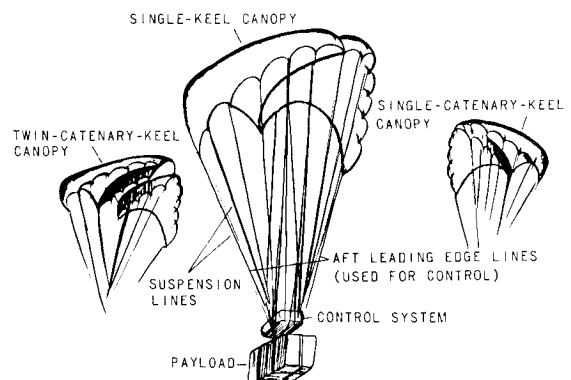


Fig. 1 Parawing precision aerial delivery system.

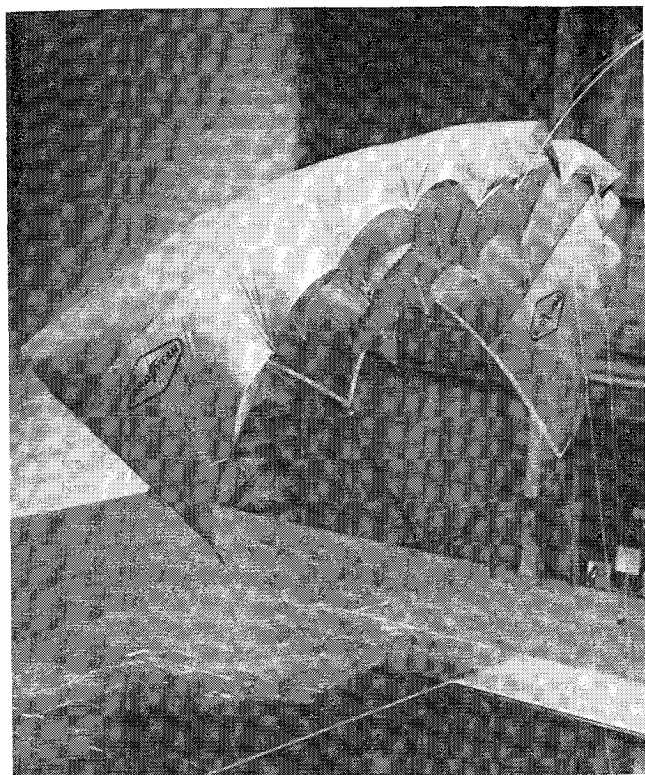


Fig. 2 Full-scale wind-tunnel trim test of twin-catenary-keel parawing.

with wing loadings from 1.4 to 4.05 psf on five parawing configurations. A pivoted dummy control system simulating actual flight conditions was used to trim the system for the free-flight tests. Only minor adjustments of the two suspension lines used for controlling the parawing were required for free-flight operation of the system. The data obtained during the wind-tunnel tests are shown in Figs. 3 and 4. Lift and drag coefficients obtained during the tests are overlaid on data previously obtained from 15-ft parawings in the same wind tunnel.

Two techniques used to obtain L/D of free-flight models in still air are shown in Fig. 5. Both photographs were taken of the same test. One photograph is a time exposure to indicate the flight path as a blurred line; the second, a composite of two frames of motion-picture film taken approximately 1 sec apart. The test was conducted in the Goodyear Aerospace airdock, which affords a floor-to-ceiling clearance of approximately 180 ft.

In general, the operating envelope of the parawing system is as shown in Fig. 6. To accomplish the mission for which the system is intended, a glide ratio of at least 2 to 1 and a

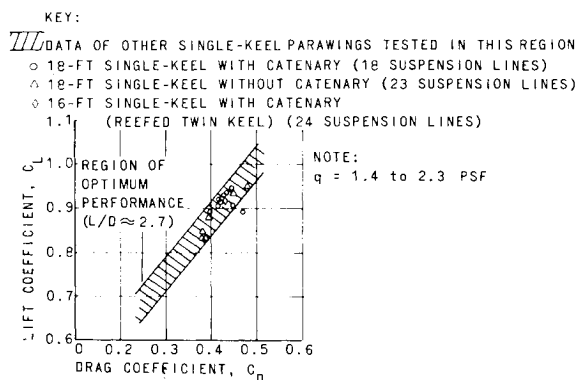


Fig. 3 Single-keel parawing wind-tunnel test results.

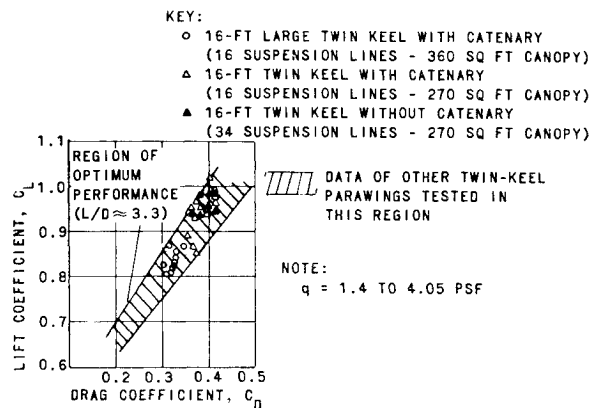


Fig. 4 Twin-keel parawing wind-tunnel test results.

descent rate not exceeding 25 fps is desirable. The 25-fps maximum descent rate is necessary to permit a landing impact comparable to parachute delivery, whereas the high L/D and high glide velocity are desirable to penetrate winds.

The PPADS is controlled entirely by changing the length of the aft leading edge lines (see Figs. 7 and 8). The amount of length change required is directly proportional to the force required to pull the line in and inversely proportional to the turning radius desired for the parawing. Data obtained during flight tests were used in determining the bank angle in conjunction with the following analytical technique.

Turning radius and time to turn  $360^\circ$  may be computed from the following equations:

$$R = V^2 / g \tan \phi \quad (1)$$

$$t = 2\pi R / V \quad (2)$$

The turning radius and time to turn  $360^\circ$  are plotted in Figs. 9 and 10 against glide velocities for various bank angles. The maximum bank or roll angle is assumed to be  $50^\circ$ .



Fig. 5 Photographic methods for obtaining L/D.

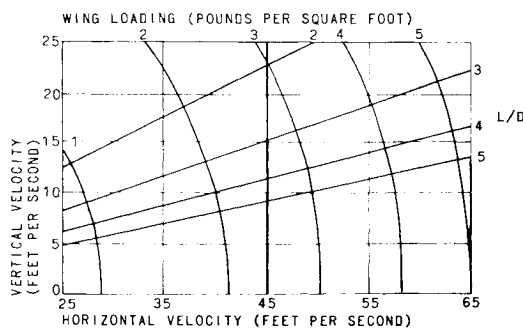


Fig. 6 Parawing operating envelope.

### Stress Analyses

Stress analyses were conducted for the single- and twin-keel parawing systems defined in Table 1.

Deployment is a major consideration because the deployment condition is critical for most structural elements; the weight of the system, therefore, is governed by deployment-stress requirements.

The parawing inflation time may be predicted by

$$t_f = 2.5 L_R/V \quad (3)$$

where 2.5 is an empirical constant, and  $V$ , the deployment velocity. The total force is given by

$$R = SgC_R \quad (4)$$

Preliminary tests showed  $C_R$  to be 3.0.

Figure 11 graphs the relationship between the deployment velocity, the wing loading, and the maximum  $g$  loading for systems without reefing. For example, with a payload weight of 500 lb and a deployment velocity of 150 knots (253.5 fps), the resulting load is 38,000 lb for an assumed wing loading of 3 psf, a load factor of 76  $g$ .

This computation results in a high value because it was based on wind-tunnel test data and corresponds to an infinite payload mass. Figure 11 and the calculation are for the worst condition, that is, without reefing. Reefing techniques using single-stage techniques have reduced the opening shock by at least 75%. The final reefing technique developed incorporates a zero-length reefing line encompassing all of the suspension lines located at a distance from the payload equivalent to the length of the shortest suspension line. In addition, the four nose lines are pulled in to effectively provide a  $\frac{3}{4}$  nose tuck.

### Guidance and Control

Two methods may be employed for guidance and control of parawing systems: 1) displacement of the suspension lines and 2) addition of a drag device. Most systems with all-flexible parawings use various forms of line-length adjustment. PPADS uses the method developed at the outset of parawing development, that of adjusting the length of the rear leading edge lines to afford directional control.

Fig. 7 Bank angle vs control-line retraction.

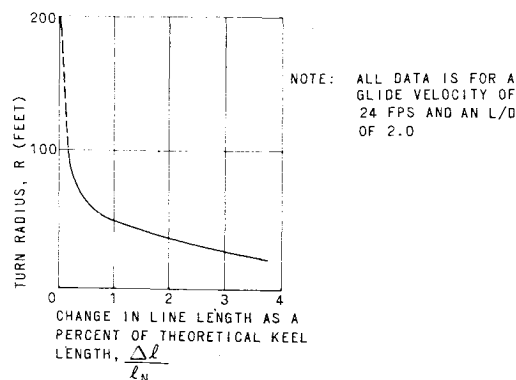
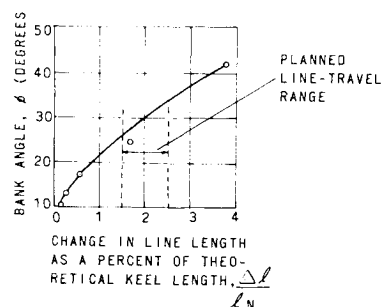


Fig. 8 Radius of turn vs control-line retraction.

Fig. 9 Turn radii vs glide velocities.

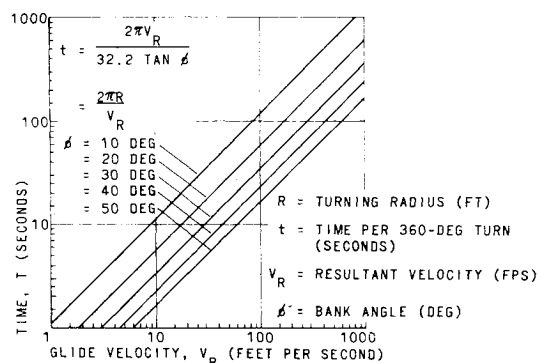
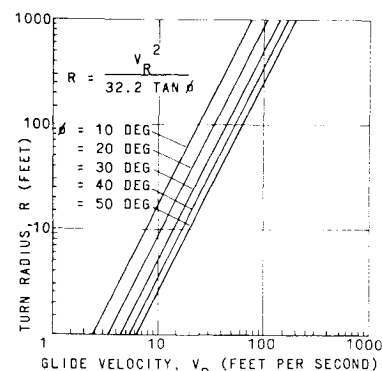


Fig. 10 Turn time vs glide velocities.

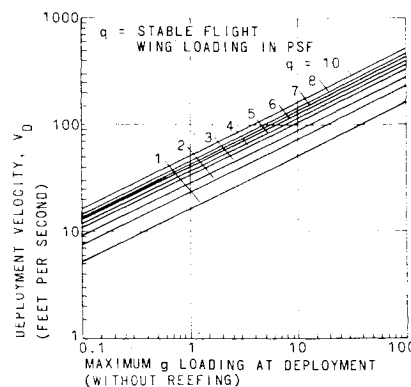


Fig. 11 Deployment velocity vs loading.

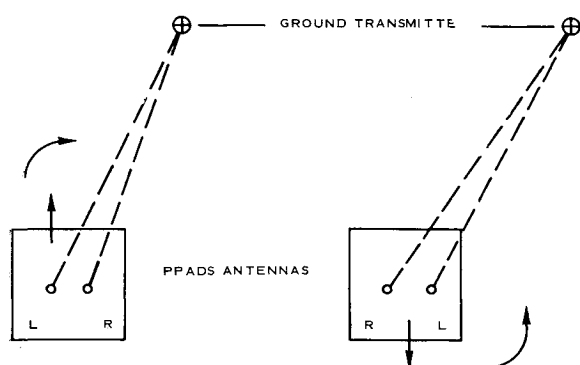


Fig. 12 PPADS homing guidance.

The guidance and control system is designed to operate as an integral part of the PPADS. It uses radio receivers as onboard equipment and matching transmitters as ground homing stations. If the rf signal is lost, as when passing over the target transmitter, the system will automatically apply a control force to produce a preset turning rate. The vehicle will fly a helical path to ground unless the signal is again received. To delay activation of this circuit in the event of short-duration signal losses, a 0.25-sec time-delay relay is inserted between the amplifier and the relay.

Although the system appears to be susceptible to a  $180^\circ$  ambiguity, no practical ambiguity exists. The system is designed to recognize which antenna is receiving the greater modulation signal and to turn toward the stronger signal. As illustrated in Fig. 12, the system will fly toward the homing beacon regardless of initial heading.

The number of degrees of deviation from the  $180^\circ$  axis that are required to provide sufficient signal differences to be recognized by the control system depends upon factors such as transmitter and receiver antenna patterns, receiver sensitivity, roll attitude, differential amplifier resolution, and resolution of the comparison circuits. The sum of the above factors could exceed  $\pm 15^\circ$ ; however, testing indicates that the system resolution is within  $\pm 5^\circ$  from the rear and the front.

This control system is being used with parawings for 100- to 500-lb payloads, but it has the capability of being used with 2000-lb-payload parawings. The control cables are required to deliver a maximum force of 24 lb for the twin-catenary-keel parawings. Within a 1-in.-diam wrap drum, the torque on the output shaft of the gear box would be  $24$  or  $30 \times \frac{1}{2}$ , or 12 to 15 in.-lb. The system includes a maximum control-line travel of 12 in.

An antenna system has been designed to provide the best comparison between directivity and receiving sensitivity.

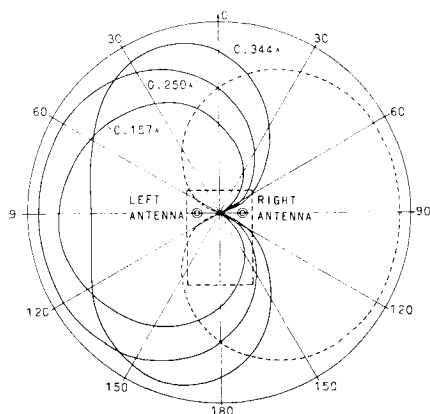


Fig. 13 Homing antenna signal sensitivity.

The antennas consist of the two quarter-wave elements on the mounting plate including quarter-wave electrical loop, rf switch, matching networks, and cables.

At the switching rate, the antenna pattern is essentially a cardioid homing pattern directed to the right or left side of the perpendicular line joining the antennas in the horizontal plane. The homing signal sensitivity, assuming a cardioid pattern as shown in Fig. 13, is proportional to the sine  $(\pi S/\lambda)$ , where  $S/\lambda$  is the space between the two antenna elements in wavelengths.

The electrical length, in wavelengths, of the loop termination between the two antennas is equal to the space dimension. The rf switch supplies a single-ended output for the receiver and eliminates the need for two rf amplifiers. A spacing of  $0.25\lambda$  provides an ideal design compromise in sensitivity by giving an output differential signal change of 2.5 db for a  $10^\circ$  pointing error.

To operate at frequencies sufficiently high to remove interference from the ground, a one-to-three scale model version of the antennas and the payload box was designed and fabricated. Pattern measurements were made on the antenna range at Goodyear Aerospace's Wingfoot Lake facility. Both vertical and horizontal patterns were taken, including tests for VSWR, impedance match, and equal gain at the boresight position for right- and left-hand patterns.

## Validation through Flight Testing

### PPADS for 500- to 2000-lb Payload

Twin-catenary-keel parawings were tested during September, October, and November 1967, at USAAVLABS, Fort Eustis, Virginia, and at Naval Air Facility, El Centro, California. The parawings, with planform areas of 609 ft<sup>2</sup> (305 ft<sup>2</sup> when reefed to the single-keel configuration) had keel lengths of 21 ft. One of the parawings, rigged with nylon lines, weighed 88 lb; the other, rigged with steel lines, weighed 108 lb.

The parawings were designed for 150-knot deployment shock loads while carrying up to 2000 lb of cargo without reefing. Talon no. 09 zippers were installed along the keels to reef the parawings to the single-keel mode. These were replaced with daisy-chain fasteners due to the repetitive nature of the testing and the wear on the quick-release retainer and pin fittings caused by deployment shock. For regular field service, the zipper reduces packing time almost 50%.

Five flights were conducted at Fort Eustis to check preliminary rigging and trim-out. All deployments were success-

Table 1 Systems definition

Item	Single keel	Twin keel
Wing planform area	220 ft <sup>2</sup>	275 ft <sup>2</sup>
Theoretical keel length	18 ft	16 ft
Maximum wing loading	2.7 psf	2.7 psf
Fabric tensile strength required, warp and fill	135 lb/in.	120 lb/in.
Minimum strip tensile with a factor of safety = 3/1; $T_F = 7.19 \times 10^{-5} L_K F_S V_D^2$ , where $T_F$ is the tensile strength of fabric, $L_K$ is the theoretical keel length, $F_S$ is the factor of safety, and $V_D$ is the deployment velocity		
Resultant velocity of system in flight	48.75 fps	48.75 fps
Vertical descent rate with $L/D = 2$	21.8 fps	...
Vertical descent rate with $L/D = 3$	...	15.4 fps

ful and a reasonably good rigging for both single- and twin-wheel modes was obtained.

Fourteen tests were conducted at El Centro to demonstrate deployment and performance capability. All tests were considered successful relative to the packing and deployment approach. The parawing demonstrated its structural capability through the complete test envelope including deployment of a 2000-lb payload at speeds up to 150 knots.

During the flights at Fort Eustis and El Centro average glide ratios of 2.8 were attained with a 500-lb payload; a maximum L/D of 3.3 was recorded. Addition of the control box did not significantly affect the performance of the system. Increasing the payload to 2000 lb and increasing the payload size proportionally added noticeable drag to the system and reduced the L/D approximately 10%.

Vertical descent rate was the minimum (approximately 15.6 fps) on a straight flight path with a 500-lb payload. It was approximately 30 fps with a 2000-lb payload. Increases in the vertical descent rate also were observed as the turning radius was reduced and as the angle of bank increased. For example, the vertical descent rate increased to 15.7 fps on a 150-ft radius at a 6° bank angle and to 16.2 fps on a 90-ft radius at a 15° bank angle.

No failures resulted from packaging or deployment of the parawings during the 19 flights at Fort Eustis and El Centro. The tests demonstrated a reliability and confidence level of approximately 90% for the tested parawing design characteristics and indicated that the parawing system can be delivered, flown, refurbished, and handled in the field by existing aircraft, equipment, and parachute riggers.

#### PPADS for 500-lb Payload

##### General

The parawing precision aerial delivery system is designed to meet the following performance requirements and objectives: 1) payload capacity of 100 to 500 lb, 2) minimum effective glide ratio of 2.4 to 1.0 (1.8 to 1 required) when operating in the automatic homing mode on straight track toward the ground transmitter, 3) deployment from 500 to 30,000 ft from any type of aircraft at velocities from 0 to 150 IAS, 4) maximum turn radius of 100 ft in either direction, 5) command control from a ground station to a landing within 100 ft of a desired point in winds up to 75% of the forward air speed, 6) automatic homing with a CEP of 200 ft of a ground-based transmitter in winds up to 15 knots, 7) vertical descent rate at impact of 25 fps or less, 8) mission duration of 45 min nor-

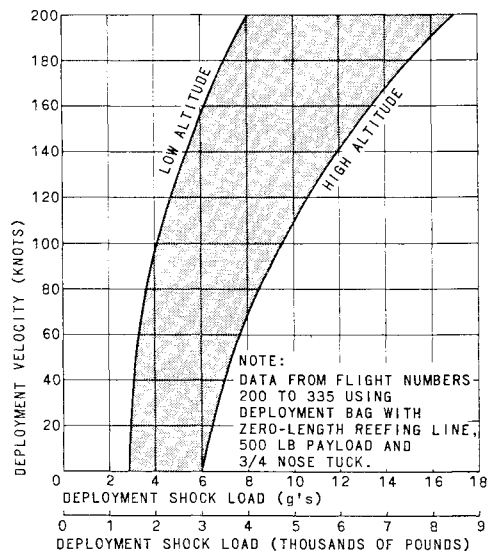


Fig. 14 Final PPADS test results.

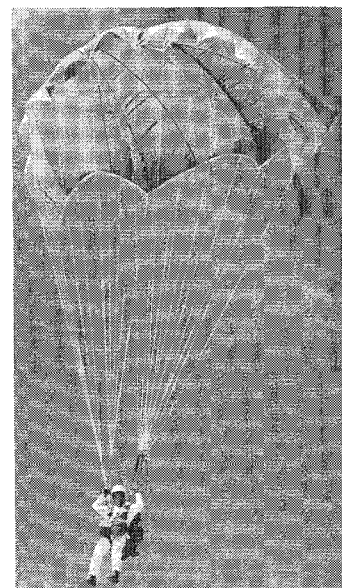


Fig. 15 Manned parawing flight.

mal operation in the automatic homing mode, 9) cargo attachment and preflight check within 7 min, and 10) turnaround time, not including time en route, within 65 min. A testing program was conducted to confirm that the PPADS meets these requirements and objectives. Most of the tests have been conducted by Goodyear Aerospace at Yuma Proving Ground, Yuma, Arizona.

##### Operational Description

The PPADS parawing weighs approximately 35 lb, including suspension lines, and packs in less than 2 ft<sup>3</sup>, including the deployment bag. To prepare the system for flight, four connections of riser-line groups, two control-line attachments, and one antenna release-line attachment are made between the parawing and the control subsystem. The parawing is packaged on top of the control subsystem prior to flight.

The control subsystem is contained in a 20-in. × 21-in. × 7-in. metal box and weighs approximately 65 lb. The control subsystem housing has four fastener locations for the four groups of riser lines and the four payload-carrying straps. System shock loads are carried by the lines and straps, not by the control subsystem. The only other protrusions from the control subsystem housing are the antennas. The antennas are spring-loaded to prevent damage during landing and to permit retraction prior to the deployment sequence.

After the payload is dropped from the aircraft, the PPADS deployment sequence is initiated by a static line attached to the drop aircraft. Break cords rupture and permit the system to play out while maintaining proper orientation with the parawing, which remains packed in its deployment bag.

The deployment bag requires a deployment force of at least 50 lb. As the parawing deploys from the bag, the system is properly oriented, payload first, control subsystem next, then the riser lines up to the parawing. When the parawing separates from the deployment bag, the reefed parawing deploys.

Four seconds after deployment, the transition from reefing mode to trimmed-flight mode takes place with the parawing trimmed for flight in a 100-ft-radius right turn to seek the transmitter. Six seconds after deployment, the servocontrol motor activates to steer the parawing to the target.

The reversible servocontrol motor is connected by secondary lines to the aft leading-edge lines; a windup drum on the output shaft of the motor takes up and releases line to steer the parawing. The motor may be controlled by either the automatic homing guidance or the remote manual system. Upon impact with the earth, the payload quick-release dis-

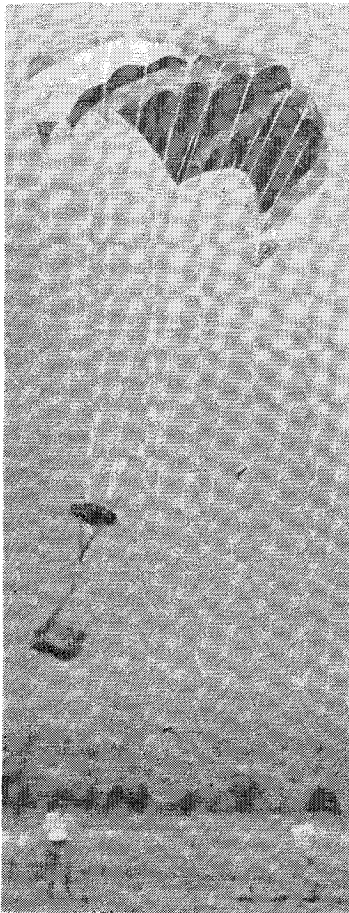


**Fig. 16 Final PPADS system.**

connects the payload and the control subsystem is turned off as the antennas are retracted.

#### **Test Program**

One week of preliminary testing for evaluation of wing trim was conducted at the NASA-LRC full-scale wind tunnel to evaluate the twin- vs single-keel parawings with and without catenary keel panels. The testing was conducted June 1-15, 1968.

The field test program at Yuma Proving Grounds was divided into four phases. The duration of each phase depended on the test results. The configuration and testing procedures were altered as required to meet the objectives of the test phase.

The objective of phase I tests was to determine the maximum  $g$  loading on the payload through a series of reefing techniques including: 1) no reefing, 2) simple tie of the rear three or four parawing lines (the last line of each leading edge and keel), 3) attachment of reefing line around periphery of parawing forming the two leading edges into a circle during deployment, 4) attachment of reefing line as in 3, plus a daisy-chain closure of the trailing edges to totally encapsulate the air trapped during the initial inflation, 5) use of the Snyder reefing or wrapping flap to slow the deployment of the parawing by releasing the lines slowly, 6) use of a zero-length reefing line plus various nose tucks, and 7) center-keel line retraction to reduce the deployment shock load. The test series evaluated the deployment  $g$  loading on the single- and twin-keel parawing configuration. A manual mechanical  $g$  load indicator was the only instrumentation required for this phase. Variations of both configurations were flown and their performance characteristics were evaluated. The variations included the use of catenary keel panels for better aerodynamic performance and greater lateral stability with fewer suspension lines. The twin-keel parawing was evaluated for optimum performance and maximum L/D, with the

ultimate L/D goal of 3 to 1. The sixth technique consistently produced the desired performance characteristics. Figure 14 is a compilation of the results of final system testing.

Manned parawing jumps were used for rapid data collection and performance evaluation of the various configurations. The cooperation of the U.S. Army Golden Knights parachute team (Sgts. R. Morgan and J. Phillips) and the USAAVLABS test jumper (Sgt. J. Rodriguez) is gratefully acknowledged. Figure 15 shows Sgt. Rodriguez flying a twin-catenary-keel parawing during this phase of the test program.

Instrumentation and the control subsystem were included in the phase II tests to obtain performance data. Remote manual guidance of the system was used to obtain glide ratio, turning radius, velocity at impact, payload weight variance, parawing configuration modification, and performance effects of the catenary keel panels.

The twin-catenary-keel parawing outperformed the other parawing variations. In flight, it exhibited the characteristic of a solid flying wing with no sideslip, even in turns as tight as  $360^\circ$  in 3 sec. Although this parawing exhibits an L/D 22% greater than the single-keel parawing, it requires 20 to 30% less force to produce equivalent turns. The final system just prior to landing is shown in Fig. 16.

The following rigging line materials were evaluated: 1) aircraft cable (steel used as a control sample), 2) braided nylon lines, 3) dacron-polypropylene lines, and 4) dacron lines. Material 3 evolved as the best tradeoff between line stretch and recovery, temperature and humidity effects, and weight and mass relationships.

Phase III tests evaluated the total system performance. Both remote manual guidance and automatic homing operations were tested. Automatic homing tests evaluated effective L/D, vertical descent velocity at impact, and the capability of attaining a 200-ft CEP. Flights were made with varying payload weights and various deployment velocities to cover the entire performance envelope.

Phase III results are: 1) successful flights with deployment at altitudes from 500 to 24,000 ft at velocities from 0 to 150 knots IAS with payload weights from 100 to 500 lb, 2) turning

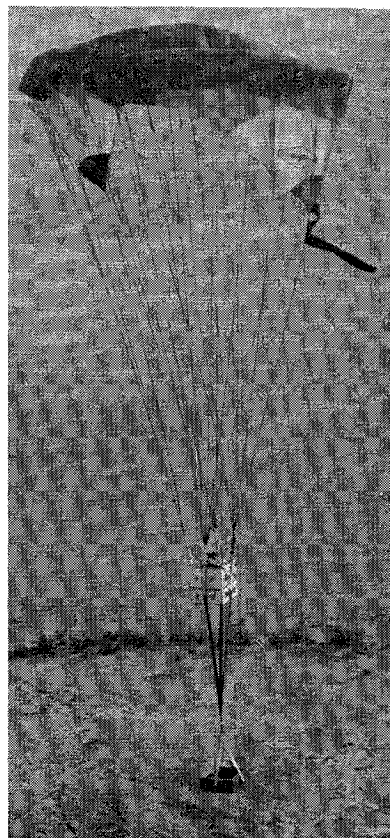


**Fig. 17 PPADS with instrumentation.**

radii less than 100 ft, 3) effective L/D's of 2.57 in the automatic homing mode, 4) checkout and turnaround time of less than 45 min, and 5) CEP of 100 ft for manual flights.

Phase IV included the reliability tests, demonstration, and evaluation program. Eleven tests were conducted at maximum conditions within the operational envelope already established. The tests included a deployment altitude of 15,000 ft, a deployment speed of 150 knots, and an equivalent payload weight of 500 lb. The launching aircraft deployed the system from downwind, upwind, both sides, cross wind, and directly over the target. Phase IV testing obtained overall system reliability and maintainability data, a CEP of 187 ft, and the following final system performance data.

The flight test performance met or exceeded all contract requirements. At least  $\frac{2}{3}$  of the deliveries on automatic homing landed within 200 ft of the target. Manually controlled flights averaged 66 ft from the target with none in excess of 100 ft. A standoff release capability of 2.5 to 1 was demonstrated, and maximum glide ratios of 3.3 were attained.

Payload weights from 100 to 500 lb were flown with no rigging changes required. Vertical descent rates averaged 20 to 22 fps with 500 lb payloads. The parawing system proved highly maneuverable, requiring relatively small control movements and forces. It was possible to make turns as small as 20-ft radius using only a 9-in. control line adjustment and a 25-lb force. In normal operations, a 60-ft-radius turn required only a 3-in. control-line adjustment and a 12-lb force.

Deployment shock loads using 500 lb payloads dropped from up to 24,000 ft at 150 knots IAS averaged 7 g's with a maximum of 12 g's recorded. A total of 322 flights were conducted including 49 manned jumps, 15 manually controlled flights, 36 automatic homing flights, and 14 instrumented flights.

Instrumentation for phase IV was to determine the cause of any malfunction or performance deviation. The tests included photograph coverage from onboard the PPADS system, from the ground, and from the deployment aircraft. The payload was reduced in weight by an amount equivalent to the onboard instrumentation so that the system performance could be properly evaluated. The instrumentation system was mounted on top of the control box as shown in Fig. 17.

The onboard instrumentation system used continuous and time-sharing techniques (via a commutator) to permit recording of all data items including: 1) maximum shock load at deployment, 2) relay closure events including left and right turn, homing, and loss of carrier signal, 3) amplifier input signal control voltage, 4) feedback potentiometer voltage, 5) servo battery voltage, 6) instrumentation battery voltage, 7) receiver battery voltage, 8) timing signal, 9) control-box roll and pitch angle, 10) control-box support cable loads during steady-state flight (no capability for obtaining deployment shock loads), 11) servomotor current, 12) control-cable loads during steady-state operation (no capability for obtaining deployment shock loads), 13) control-cable position.

An onboard wind-angle-lens 16-mm motion picture camera was used on a portion of the flights to evaluate the opening performance of the parawing during various reefing and deployment configurations. Smoke bombs were attached to some flights to aid the recording of flight path vs applied control force and the determination of radius of turns.

The onboard instrumentation system is supplemented by the use of a Fairchild analyzer. The Fairchild analyzer is used to determine the effective and actual L/D's of the system during flight. By flying the system along the prescribed

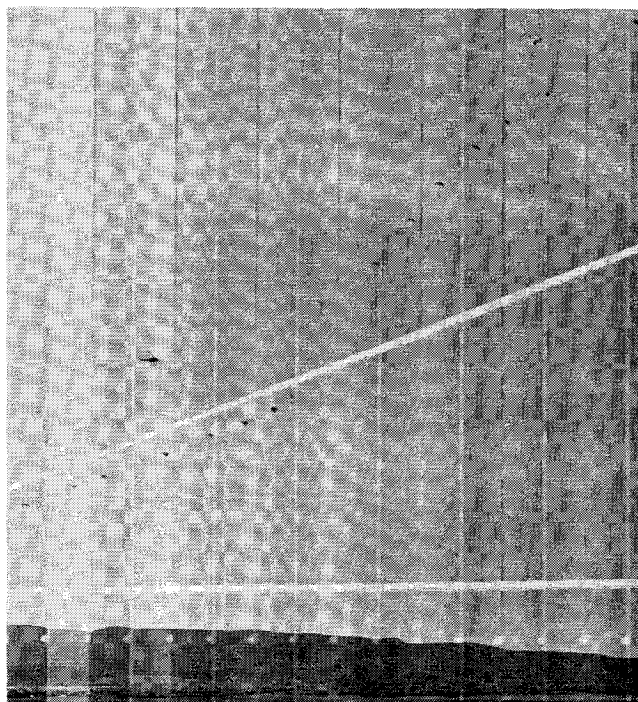


Fig. 18 Fairchild analyzer data.

course both upwind and downwind, the results can be averaged to obtain the L/D and the descent rate.

The course for use of the Fairchild analyzer is laid out by simple geometry depending on the portion of the flight to be recorded. The record obtained, due to the method of operation of the analyzer, can be read by the use of an overlay to spot check the L/D and descent rate of the system.

In a panning motion-picture or theodolite camera, both the lens and the film plane rotate. The recorded image is foreshortened, and, because the object-to-lens distance constantly varies, the image size also varies. The Fairchild analyzer operates as a focal-plane shutter taking vertical, thin photographs across the negative from one side to the other; the lens and film are fixed. Therefore, the recorded image size and scale of movement are constant. Figure 18 shows a sample of the type of data produced by the Fairchild analyzer.

## Conclusions

The parawing precision aerial delivery system has proven its capability to deliver cargo to a predetermined landing site automatically. The in-house work at USAAVLABS and the industry work supported by the Army all have been essential elements in the successful development of the system to its current state.

Deployable wing systems have made great strides in providing entirely new capabilities in diverse areas. Their impact is such that this must be recognized as a separate area of technology. Although considerable effort has been and is being expended in this field, there is still much to be done. Development of optimum materials for the canopy and the suspension lines, study of canopy planform shapes, payload protection devices, steering technique optimization, value-engineered control systems, reefing techniques, and flaring technique development are some of the areas which need additional effort for improvement of current configurations.